Journal of Chromatography A, 1598 (2019) 163–174

Contents lists available at ScienceDirect

Journal of Chromatography A

journal homepage: www.elsevier.com/locate/chroma

Advances in offline approaches for trace measurements of complex organic compound mixtures via soft ionization and high-resolution tandem mass spectrometry

Peeyush Khare[a], Aurelie Marcotte[a,1], Roger Sheu[a], Anna N. Walsh[b,c,2], Jenna C. Ditto[a], Drew R. Gentner[a,*]

[a] Department of Chemical and Environmental Engineering, Yale University, New Haven, CT-06511, USA
[b] Department of Marine Chemistry and Geochemistry, Woods Hole Oceanographic Institution, Woods Hole, MA 02543
[c] Department of Civil and Environmental Engineering, Massachusetts Institute of Technology, Cambridge, MA 02139

ARTICLE INFO

Article history:
Received 29 November 2018
Received in revised form 18 March 2019
Accepted 19 March 2019
Available online 19 March 2019

Keywords:
Air quality
Time of flight mass spectrometry
Gas chromatography with tandem mass spectrometry
Semivolatile organic compounds
Organic aerosol

ABSTRACT

Complex airborne mixtures of organic compounds can contain 10,000′s of diverse compounds at trace concentrations. Here, we incorporate high-resolution mass spectrometry into our integrated offline sampling-to-analysis measurement system for routine molecular-level speciation of complex mixtures in gas- or particle-phase samples with detection limits of 2–20 pg L^{-1} (i.e. 0.2–1.9 ppt in 6 L samples). Analytes desorbed from custom adsorbent tubes (or filter extracts) were separated via gas chromatography (GC) and simultaneously analyzed by an electron ionization quadrupole mass spectrometer (EI-MS), and by atmospheric pressure chemical ionization (APCI) combined with a high-resolution quadrupole time-of-flight mass spectrometer (Q-TOF) with a resolution of 25,000–40,000 M/ΔM in HR-TOF and MS/MS modes. We demonstrated our system with simple standards, a Macondo crude oil standard as a reference for complex mixtures of common airborne compounds, and ambient samples using GC-TOF and GC–MS/MS. We speciated complex mixtures at mass accuracy error (i.e. mass tolerance) down to 8 ± 2 ppm (e.g. resolving analytes of mass 270.000 u with 0.003 u accuracy) using a targeted approach with 3000 molecular formulas, including hydrocarbons and functionalized analytes containing oxygen, sulfur, nitrogen, or phosphorous. This extended from compounds with 10 to 32 carbon atoms and up to 16 hydrocarbon formulas per carbon number, and a similar range for functionalized compound classes. We also demonstrated our MS/MS capabilities to differentiate structural isomers and determine the presence of specific functional groups; and our direct-TOF capability, which bypasses high-temperature chromatographic separation to preserve functionalized analytes.

1. Introduction

Complex mixtures of organic compounds play important roles in a variety of anthropogenic, biogenic, and engineered environments, and span the gas-, particle-, and aqueous-phases with diverse functional groups and volatilities [1,2]. Primary emissions of complex mixtures can undergo multi-generational atmospheric oxidation, and gas-phase organic mixtures are known to contribute to the formation of secondary organic aerosol (SOA; a major constituent of particulate matter less than 2.5 μm in diameter ($PM_{2.5}$)) and tropospheric ozone. One example is motor vehicle emissions, where historically-unresolvable precursors contribute over half of the total observed vehicular SOA [3,4]. Chemical speciation of such mixtures can provide crucial insights into their reactivity and dynamics in the atmosphere, thus assisting air pollution modelers and policy makers.

Mass spectrometry techniques are common for chemical speciation of atmospheric samples. There are two general ionization techniques in mass spectrometry: hard and soft ionization. In hard ionization, such as electron ionization (EI), a parent molecule is fragmented into predictable proportions of smaller ions. A major drawback of EI is the limited ability to characterize complex organic mixtures of co-eluting intermediate- and semi-volatile organic compounds (IVOCs and SVOCs), which were historically considered unresolved complex mixtures (UCMs)

* Corresponding author.
E-mail address: drew.gentner@yale.edu (D.R. Gentner).
[1] Now at: Waters Corporation, Raleigh NC-27604 USA.
[2] Now at: Woods Hole Oceanographic Institution, Woods Hole MA-02543 USA.

https://doi.org/10.1016/j.chroma.2019.03.037
0021-9673/

[5] since their similar, co-eluting molecular fragments cannot be distinguished by spectral tools/libraries. Still, EI is effective for chromatographically-separated analytes because of their compound-dependent fragmentation patterns which can be used with spectral libraries for analyte identification.

In contrast, chemical ionization occurs much closer to analytes' ionization energies and generally closer to atmospheric pressure in order to preserve the parent molecular ion (Figure S1) (e.g. atmospheric pressure chemical ionization (APCI)) [6]. This allows a chromatographically-unresolved complex mixture (i.e. UCM) of analytes to be deconvoluted via a high-resolution mass spectrometer (HR-MS) [7–11]. To enhance ionization of target analytes, a reagent ion is sometimes used to facilitate ionization (e.g. hydronium (H_3O^+), nitrate (NO_3^-), iodide (I^-)) [12–16]. Depending on its mass resolution, a HR-MS can identify different closely- or co-eluting ion masses in a UCM but has limited ability to distinguish between co-eluting isomers. Tandem MS (MS/MS) with high mass resolution can examine isomeric composition since MS/MS enables the structural characterization of analytes, especially when coupled with GC. Thus far, libraries and tools for gas chromatography (GC) with MS/MS are less developed than their EI-MS counterparts, and use of MS/MS in the atmospheric sciences has been limited [14,17,18]. Advancements in applications of MS/MS with either data -dependent or -independent workflows would reduce uncertainties in air pollution models by elucidating structural differences within volatility and polarity bins to better constrain chemical properties and transformations of complex mixtures in the atmosphere. Furthermore, simultaneous measurements using soft- and hard- ionization would be highly useful for comprehensive characterization of gas-phase atmospheric samples.

Past studies have used a variety of instrumentation for characterizing organic mixtures. Liquid chromatography coupled with electrospray ionization (LC-ESI) is effective for oxidized organic molecules [19,20] but does not efficiently ionize non-polar analytes, leaving out a large fraction of GC-amenable VOCs, IVOCs and SVOCs from common sources [21]. Other instruments such as aerosol mass spectrometers (AMS) effectively characterize bulk composition of $PM_{2.5}$ by vaporizing collected particles and measuring the fragments [17,22] but do not provide high chemical resolution. In contrast, there are fewer atmospheric chemistry studies combining GC with soft ionization HR-MS (e.g. pesticide residues [23], organic pollutants in water [24]). Existing research showcasing GC with soft ionization MS (typically at lower resolution) includes the analysis of diesel fuel, crude oil, motor oil, and organic aerosols present in ambient air or oxidation chambers [25–36]. Direct infusion (i.e. introduction) and analysis of samples via ultra-high resolution MS (e.g. Orbitrap, DART-HRMS: Direct Analysis in Real Time MS) has been done for a variety of sample media (e.g. water, soil, plasma) and also for aerosol samples via desorption-ESI (DESI) [37–40], but its coupling with gas-phase ionization sources is just now being explored [41].

Our integrated measurement system presented here is novel in the field of atmospheric chemistry with its: (a) use of our GC-TOF at 25,000–40,000 M/ΔM that exceeds most HR-TOFs used in atmospheric chemistry, (b) application to gas-phase (and particle-phase) organic compounds in atmospheric samples, (c) tandem MS for isomeric deconvolution and structural characterization, (d) direct-TOF analysis of thermally-desorbed analytes without GC separation in addition to the GC-TOF analysis, (e) incorporation into our integrated sampling-to-analysis system for routine offline measurements generally at sub-ppt LODs (see [42]), and (f) simultaneous analysis of GC effluent via both soft ionization HR-TOF and EI-MS.

Our aim in this work is to advance capabilities for the offline characterization of complex mixtures of gas-phase (and particle-phase) organic compounds over a wide volatility and polarity range through the application of APCI-Q-TOF in two modes: HR-TOF and MS/MS to provide information on molecular formulas and structures. Specifically, in this manuscript, we (a) present the instrument design, sample analysis, and data analysis approaches related to the integration of the APCI-Q-TOF into our offline thermal desorption (TD)- and GC-based integrated sampling-to-analysis system; (b) demonstrate and evaluate instrument and data analysis performance using standards, including a NIST crude oil reference mixture; and (c) present sample data from common airborne complex mixtures to demonstrate GC-TOF and targeted MS/MS.

2. Materials and methods

2.1. System description

2.1.1. Overview

Gas-phase atmospheric samples were collected on custom-made multi-bed adsorbent tubes as detailed in Sheu et al. [42]. As shown in Fig. 1, the thermally-desorbed sample was injected onto the GC column via a Markes TD-100. The effluent from the GC (Agilent 7890B) was split between the Agilent 6550 iFunnel atmospheric pressure chemical ionization-quadrupole time-of-flight MS (i.e. APCI-Q-TOF) and a traditional vacuum (EI)-quadrupole MS (EI-MS, Agilent 5977B). This dual-MS setup allows us to collect a more comprehensive suite of data using both soft ionization to examine parent ions and EI-MS for fragmented ions (Figs. 2, S4 and S10). In this study, we focused primarily on the integration and application of APCI with Q-TOF in HR-TOF and MS/MS modes, while the use of EI-MS is discussed elsewhere [42]. An alternative path from the TD is direct analysis (i.e. direct-TOF) bypassing the GC column with analyte infusion directly into the APCI-Q-TOF. The direct-TOF channel as part of our instrumentation is demonstrated here and will be used in future analyses to look for relevant analytes in targeted studies.

2.1.2. Thermal desorption

In normal GC-APCI-Q-TOF operation, adsorbent tubes were desorbed as detailed in Sheu et al. [42]. The full sample was concentrated on a cold trap maintained at -10 °C before it was rapidly heated to 325 °C to transfer analytes to a DB-5-MS GC column (30 m x 250 μm x 0.25 μm) for separation. When doing direct-TOF in addition to normal GC operation, samples were split during tube desorption. The analytes for direct-TOF were transferred via a passivated (AMCX) 316 stainless steel transfer line maintained at 75 °C connected directly to the APCI Q-TOF (i.e. direct-TOF, direct-MS/MS) [43]. By controlling the desorption temperature, the TD can preserve the molecular structure of thermally-labile or other highly-reactive organic compounds, which could otherwise fragment or react at high temperatures inside either the cold trap or GC column

2.1.3. Liquid standard injections

For liquid injections onto the GC column, a Gerstel cooled liquid injection system (CIS) combined with a liquid autosampler was used. The liquid injections were performed in solvent-vent mode. The glass wool inlet liner inside the CIS was held at -100 °C during sample introduction into the inlet. It was then heated at a rate of 12 °C s^{-1} and held at a maximum temperature of 325 °C for 10 min while transferring sample onto the GC column in splitless mode using helium carrier gas. A flow of 100 ml min^{-1} was maintained through the inlet to CIS vent during liquid injection onto the inlet liner. During the subsequent splitless desorption from the CIS, a column flow of 2 ml min^{-1} was maintained, after which a purge flow of 20 ml min^{-1} was maintained through the inlet and vented until the end of the GC run.

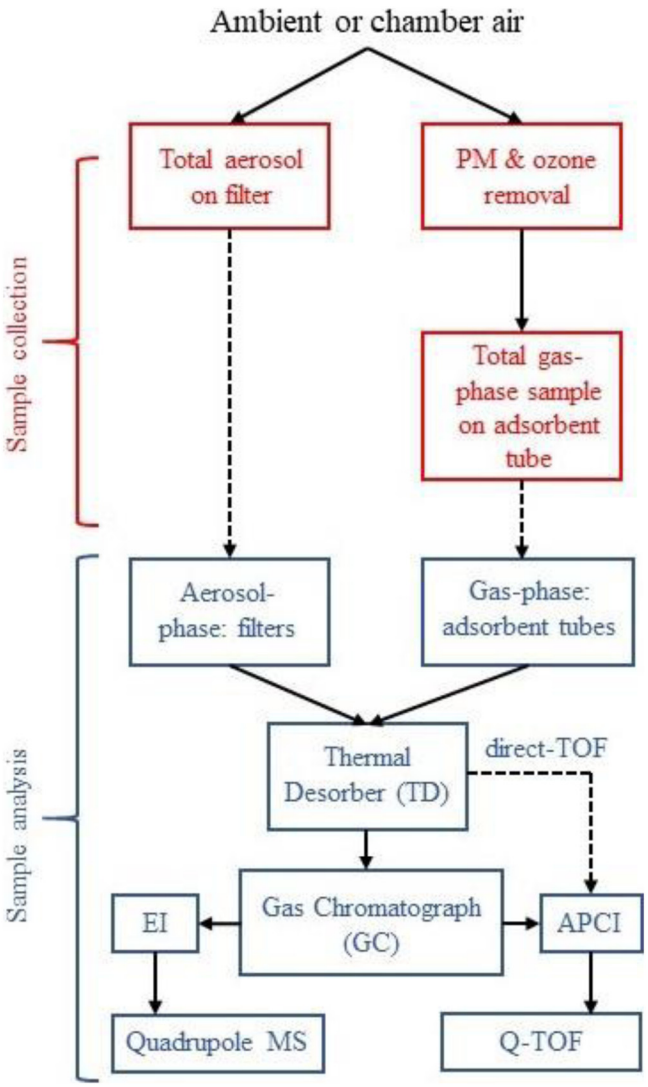

Fig. 1. A simplified diagram of instrumentation where gas-phase samples are introduced via custom packed adsorbent tubes. Introducing aerosol filter segments, or liquid injection of filter extracts directly into the GC are also possible but are outside the scope of this paper. Samples are thermally desorbed, focused, and injected into the GC column (according to temperature profile inset), which is then split between 2 MSs after separation: a traditional electron impact vacuum MS and a Q-TOF tandem MS with soft chemical ionization at atmospheric pressure and MS/MS capabilities. The instrument also includes a direct-TOF option that goes directly from desorption to MS analysis.

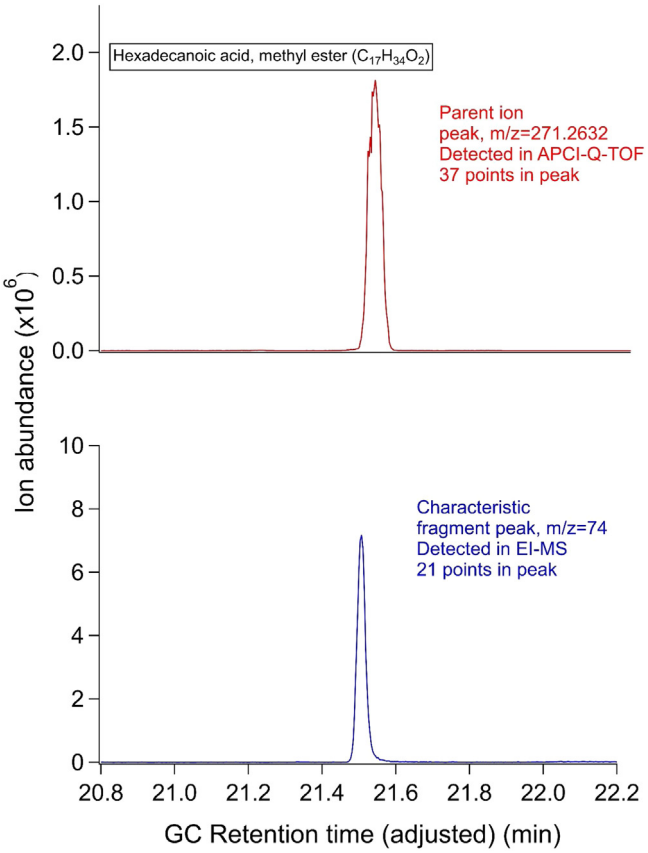

Fig. 2. Simultaneous measurements via soft ionization APCI-Q-TOF and traditional vacuum EI-MS via splitting GC column eluent enables coincident TOF measurement of preserved parent molecule (and MS/MS characterization) and use of traditional EI-MS to enhance identification and quantification capabilities. The figure shows stacked single ion chromatograms for hexadecanoic acid, methyl ester on *m/z* 271.2632 (APCI) and *m/z* 74 (EI-MS).

2.1.4. GC-separated analysis

The desorbed sample from TD was transferred to the GC column via a 0.25 mm deactivated fused silica transfer line maintained at 200 °C. The GC was held at 40 °C for 2 min before ramping at 7 °C min^{-1} to 225 °C (5 min hold) and then at 15 °C min^{-1} to 325 °C (no hold). A two-way splitter with makeup gas splits eluents 1:1 between two 0.1 mm ID, 2 m and 1.7 m deactivated fused silica transfer lines going into the EI-MS and Q-TOF, respectively. The system is also able to analyze filter samples, either by thermal desorption of filter punches in the TD or by direct injection of filter extracts (i.e. filters extracted into solvent) into the GC inlet.

2.1.5. Detection using dual MS

The analyte flow in our system was most often split between the Q-TOF and EI-MS to produce two simultaneous data streams (Fig. 2, S1 and S4). Currently, the Q-TOF uses Agilent's APCI source with a corona needle to generate reagent ions for soft chemical ionization to preserve the analyte molecular structure. Reagent ions in the ionization chamber were generated from N_2 with some residual water vapor. A detailed discussion of the observed chemical ionization pathways in our APCI chamber is presented in Section S2. We ran the APCI Q-TOF in positive mode maintaining instrument parameters within Agilent's recommended ranges: 2 μA corona needle current, 150 V fragmentor voltage and 1300 V capillary voltage. Nitrogen heated to 290 °C was used as the drying gas and set at a flowrate of 11 L min^{-1} to match vacuum flow rates in the Q-TOF. Masses were scanned at 2–6 Hz across 75–1050 m/z but are adjustable based on the application. The Agilent 6550 Q-TOF has a mass resolving capability specified at 25,000–40,000 ΔM/M, pg-level sensitivity, and down to 2 part per million (ppm) mass accuracy (i.e. ppm = difference in molecular weight/analyte molecular weight). However, analyte identification is rarely limited by the TOF's mass resolution since GC separation of analytes with similar molecular weights (Fig. 3) allows them to be detected separately by the Q-TOF. Whereas, for direct-MS (without GC) mass resolution may limit identification of all analytes in a complex mixture. Formula assignments in a targeted or untargeted analysis utilize elemental isotopic distributions to achieve high mass accuracy and improve formula confirmation or assignment (and MS/MS fragment identification when used) [44].

MS/MS analyses were performed for specific analytes with a targeted list of ions, which were selectively transmitted by the quadrupole when detected above a concentration threshold. We demonstrated the utility of targeted MS/MS through the analysis of gas-phase samples collected near downtown Atlanta, GA. The

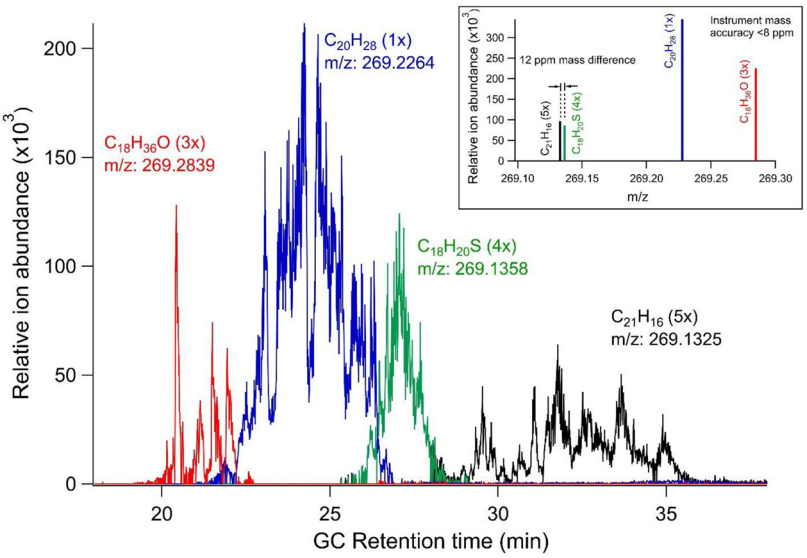

Fig. 3. Parent ion abundances measured via TOF from the Macondo crude oil standard are shown vs. GC retention time for 4 molecular formulas with very similar masses and different degrees of functionalization. Each ion mass contains a set of isomers that are partially-resolved via GC. Inset shows the *m/z* spectra of the 4 ions for comparison of mass differences. Ion abundances are magnified at 1-5x for the purposes of comparison. All ions are extracted with a mass accuracy error of 8 ppm which corresponds to an extraction window of ± 0.002 *m/z* for the ions shown.

simulated fragmentation energy (5–20 eV) was varied based on the acceleration of the ion into a collision cell, which produced a greater degree of fragmentation for higher "energies" with the degree of fragmentation depending on molecular structure. In the applications highlighted in this paper, three fixed collision energies (5, 10, and 20 eV) were tested and the resulting fragments were measured using the TOF.

2.2. Calibration

Analytical standards were used at multiple points in the instrumental system for quality control/assessment (QC/QA). Purine ($C_5H_4N_4$): *m/z* 121.0509 and HP-921 [hexakis-(^1H,^1H, ^3H-tetrafluoro-pentoxy) phosphazene] ($C_{18}H_{18}O_6N_3P_3F_{24}$): *m/z* 922.0098 were consistently applied as reference ions in the APCI interface to correct for TOF mass drift. The observed drift was within ±2 ppm for both reference ions. Additional gas-phase (Apel-Riemer) and liquid-phase (Accustandard) standards were used for calibration and testing (Table S3), and samples were spiked with internal standards to correct for instrumental mass drift across the entire integrated sampling-to-analysis system [42].

Multipoint calibrations were performed over injected standard masses ranging from 0.1 ng to 20 ng. The compound classes include: alkanes, alkenes, aromatics, terpenes, carbonyls, alcohols, fatty acid esters, phthalate esters, acetates, organophosphorus pesticides, furans and thiophenes (Table S3). The analytes in Table S3 were observed as GC peaks introduced via adsorbent tube desorption during multi-point calibrations with authentic standards or in the Macondo crude oil standard (Fig S9 and S10). Both IVOCs and SVOCs in Figure S5 showed a >90% transmission efficiency when introduced via tube thermal desorption in the Markes TD relative to liquid injection using the Gerstel cooled injection system (CIS) combined with a liquid autosampler. Numerous blanks were also employed during calibration and with the collection, transport, and storage of offline samples [38]. Calculated limits of detection (i.e. S/N = 3) for standards analyzed via soft ionization were generally around the equivalent of 1 ppt in a 6 L air sample for individual isomers, such as dimethyl naphthalene (9 pg L^{-1}), dimethyl phthalate (11 pg L^{-1}), methyl palmitate (15 pg L^{-1}), parathion (pesticide) (2 pg L^{-1}), and disulfoton (pesticide) (20 pg L^{-1}). In comparison, the LODs detected with EI-MS in this system (in Sheu et al. 2018) had a geometric mean mass loading of 9.56 ± 0.56 pg. A detailed assessment of limits of detection for our integrated system with EI-MS can be found in Sheu et al. [42].

In addition to single- and multi-component standards, the NIST Gulf of Mexico 2779 Macondo Crude Oil standard was also used in this study as a known environmental complex mixture that has been previously characterized via GC with soft ionization [31]. We analyzed it via GC-TOF through both liquid injection via an inlet onto the column and tube thermal desorption across several replicate runs. It has been comprehensively characterized by multiple institutions and instruments, and provides a consistent reference for inter-calibration of complex mixture measurements. A specific response factor for each C_xH_y compound was calculated, as the ratio of analyte abundance to the corresponding hydrocarbon analyte mass injected. Analyte mass is obtained from previous characterization that is validated against additional external references [31]. Double bond equivalents (DBE) are used to describe the breakdown of complex mixtures for C_xH_y and C_xH_yO compounds, similar to previous work [31]. Whenever possible, liquid standards are best analyzed via spiking on adsorbent tubes to most accurately recreate TD conditions for calibration. When injection of liquid standards is necessary to prevent extremely-low volatility analytes from contaminating TD transfer lines and valves (i.e. Markes TD), then care should be taken to evaluate and avoid inlet discrimination in liquid injection inlets and inconsistent response factors across wide ranges of standard volatilities. In this study, liquid injections of Macondo crude oil are used to approximate response factors of analytes injected via TD, and future studies will minimize the use of liquid calibrations. Future work in this growing area of research would benefit from the development of inter-calibration procedures with other complex mixtures connected to NIST reference materials (e.g. diesel fuel) and their precise chemical characterization across multiple instruments.

2.3. Data processing

2.3.1. GC-TOF data analysis

Agilent's MassHunter Qualitative software (version B07.0) was used for preliminary data processing. During untargeted analy-

sis, MassHunter software lists all detected chromatography peaks, peak scores, parent ion masses, and their abundance in each sample. This data can be processed for targeted or untargeted analysis [20] of a smaller set of analytes but is impractical for the characterization of complex mixtures with numerous isomers on each parent ion mass that might not necessarily be well-resolved in GC space. Therefore, we used customized code (in. NET framework) to extract raw data in batch mode for multiple two-dimensional layers (i.e. exact ion masses versus GC retention time). For each layer, we extracted targeted exact ion masses containing only elements of interest (e.g. C_xH_y, C_xH_yO, C_xH_yS, and C_xH_yN) and valid molecular formulas (exact masses determined using Agilent MassHunter software). Each layer contained a range of carbon numbers (e.g. 10–32), a fixed number of non-carbon/hydrogen atoms, and valid DBEs that extend up to DBE 15, where each DBE represents the removal of 2 hydrogen atoms via the addition of a cyclic carbon structure or a C=C double bond [11]. Since our analytical system is sensitive to mass differences on the order of a few parts per million, we were able to differentiate analytes with very similar molecular masses (Fig. 3). Extracted layers were then processed in IgorPro (using existing code from previous work), which calculated peak areas for exact masses within user-defined integration windows that we constrained based on retention indices (Figure S2) [29,31].

2.3.2. GC–MS/MS data analysis

Ion masses of interest identified during targeted and untargeted analysis were further investigated in a targeted manner by performing MS/MS to obtain fragmentation spectra at several fragmentation energies. These spectra serve as inputs to the growing number of open source programs for MS/MS structural identification. We used SIRIUS and CSI: FingerID to identify key molecular formulas and features because they have been shown to perform reliably for atmospherically relevant organic compounds [45,46]. SIRIUS uses the exact mass and isotope distributions to determine formulas. CSI: FingerID then identifies potential structures using fragmentation trees and machine learning methods [45–47]. We further checked these tools using MS/MS data from different functionalized standards including phthalates, terpenes, and amines.

The molecular formulas generated via MS/MS fragmentation spectra also validate the molecular formulas of parent ion masses determined from the TOF. While the molecular formulas are typically identical for all high-scoring hits, a variety of molecular structures can be proposed based on the fragmentation patterns. Using a set of the highest scoring results (e.g. 5–10 structures) that meet QC abundance thresholds provided more confidence in the key molecular features present, but confirmation of those features and their exact configuration would require additional analyses. External information like relative GC retention indices are one example of a useful metric to confirm the identified structural features.

3. Results and discussion

3.1. Systematic high-chemical resolution speciation of complex mixtures via GC-TOF

3.1.1. Mass accuracy

Differentiating between ion masses at high resolution is key to the chemical characterization of complex mixtures (Fig. 3). We used the NIST crude oil standard to validate the separation and mass resolving capability of our GC-APCI-Q-TOF system across a wide volatility range from VOCs up to low-volatility organic compounds (LVOCs) (Fig. 4). To demonstrate the mass resolving capability in a complex matrix with compounds that are very similar in terms of parent ion mass but different in their molecular composition, Fig. 3 shows individual ion chromatograms for a subset of compounds in the crude oil standard: $C_{18}H_{36}O$ (m/z: 269.2839), $C_{20}H_{28}$ (m/z: 269.2264), $C_{18}H_{20}S$ (m/z: 269.1358) and $C_{21}H_{16}$ (m/z: 269.1325). These hydrocarbon groups and sulfur-containing species were all reported in previous work with the NIST oil, but oxygen-containing species were not included in that study [31]. Each chromatogram shown contains numerous isomers that can be further resolved with chromatography at slower temperature ramp rates, and their degrees of branching characterized as a function of retention time [11,25,30,31,33]. A range of individual standards were used to confirm the ion masses produced via APCI. To enhance sensitivity, the masses presented here (e.g. Figs. 3–4) were extracted at 8 ppm mass tolerance. However, m/z peak centroids were accurate to 5 ppm or better for trace compounds in complex mixtures. Fig. 3's inset shows the 4 parent ion masses in mass spectral space with the separation of the 2 closest masses being only 12 ppm. This high mass resolution and accuracy, combined with GC separation enables our system to deconvolve complex mixtures of VOCs, IVOCs, SVOCs, and LVOCs in environmental samples.

3.1.2. Aliphatic and aromatic hydrocarbons: from "unresolved complex mixtures" to carbon number "bubbles" resolved by carbon number and compound class

We organized the components of complex mixtures based on the elements they contain, carbon number, and then molecular formula. We demonstrate this using the NIST crude oil standard. Fig. 4a shows the total ion chromatogram of the NIST crude oil as a characteristic example of an UCM. The compounds in the IVOC and SVOC range are dominated by C_xH_y compounds, though there are also contributions from compounds with heteroatoms (C_xH_yS, C_xH_yN, and C_xH_yO) (Fig. 5). Chromatograms for each parent ion in the C_xH_y layer are extracted from the TOF data and organized into individual "carbon bubbles" for each carbon number as shown in Fig. 4d. Each bubble is constituted by C_xH_y ions which have the same number of carbon atoms (Fig. 4b). The compounds are further separated within a carbon bubble by volatility (moving horizontally by GC retention time) and by compound class (moving vertically by selected m/z; i.e. DBE). For each downward step inside a bubble, there are two fewer H atoms (equiv. to one DBE) compared to the base linear/branched alkane. Carbon bubbles cover structural classes that range from linear/branched alkanes at DBE 0 to polycyclic aromatic hydrocarbons at DBEs $\geq$ 7. More specifically, for petroleum-related samples they are typically: 0 (linear/branched alkanes), 1–3 (cyclic alkanes), 4–6 (single-ring aromatic) and >6 (polycyclic aromatic).

There are some limitations in how DBE corresponds to structural features. The subtraction of 2 H atoms (i.e. + 1 DBE) could represent the inclusion of a C=C double bond rather than a ring. This is particularly relevant for DBEs 1–3, which could represent alkenes in fresh combustion emissions where they are more prevalent, but are unlikely to represent alkenes in crude oil. Similarly, DBE 4 could be a tetracyclic alkane rather than an aromatic compound. The sample type (e.g. petroleum) or proximity to various sources can inform the interpretation of DBEs 1–3 (e.g. mostly cycloalkanes in petroleum), but additional information can be necessary to further characterize the complex mixture. These can be tested using variations in ionization energy [31,33] or reagent ions, but in our system they can also be further characterized via MS/MS, especially with greater GC separation of isomers.

Chemical ionization at atmospheric pressure can produce a range of analyte ions depending on the reagents (or contaminants) present and the dominant ionization pathways, which can also be influenced by the structural features, proton affinity, basicity, and ionization energy of the analyte. In the Agilent APCI, linear and branched alkanes as well as cyclic alkanes (DBEs 0–3) mainly ionize via hydride abstraction (ionization chemistry discussed in SI Section S2) and are hence quantified by the abundance of $[M-H]^+$ ion ($[M]^+$ for DBE 3). Single-ring aromatics and polycyclic aromat-

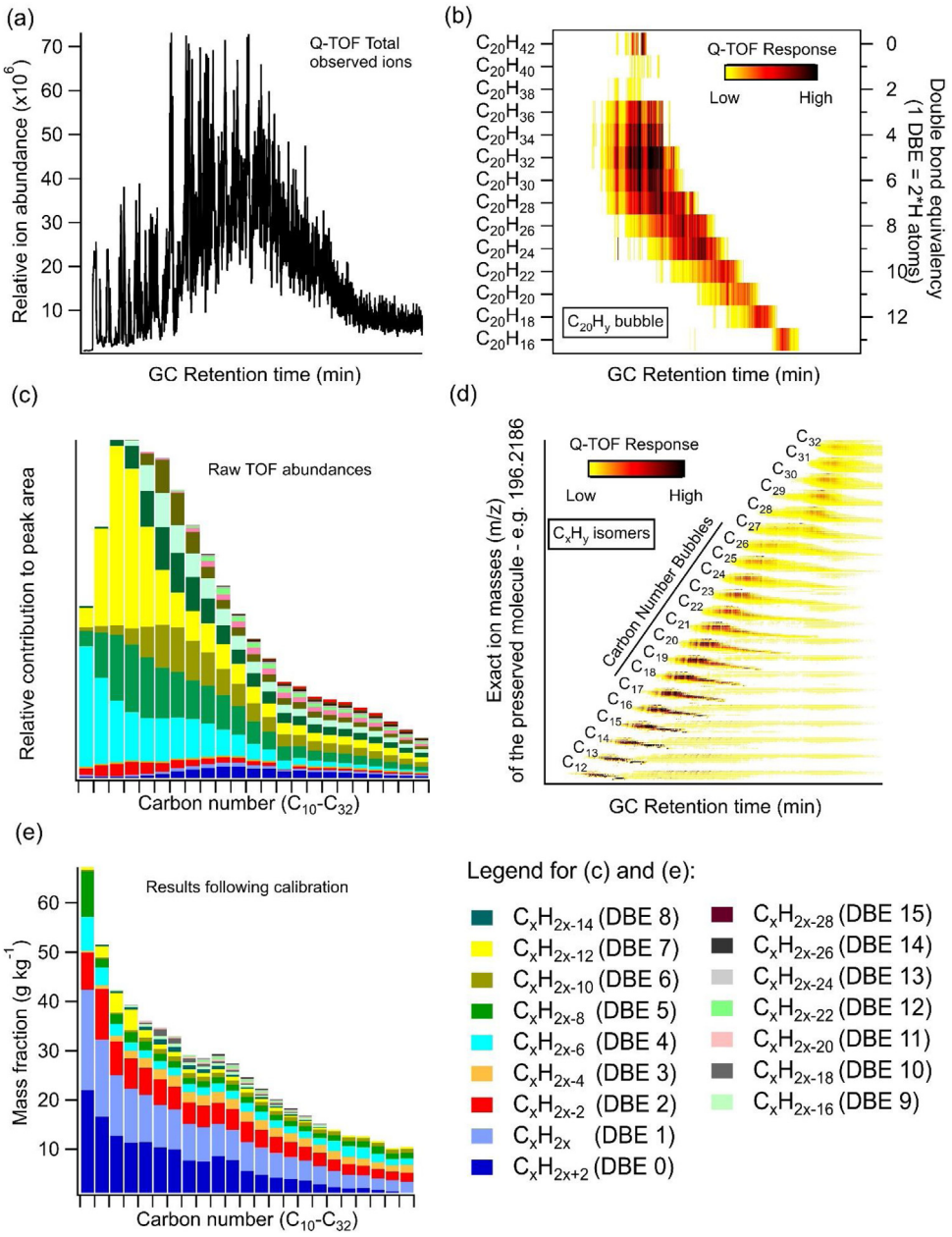

Fig. 4. Complex mixture speciation of NIST Macondo crude oil complex mixture using our TD-GC-APCI-Q-TOF system, from raw data to final product. (a) The unresolved complex mixture as a total ion chromatogram can be separated by the TOF into exact molecular masses, such as the C_{20} carbon bubble shown in (b) enlarged to show the breakdown by compound class (i.e. double bond equivalents, DBE). (c) These isomers can then be binned (i.e. integrated) by carbon number and compound class, where each segment of a bar is an exact mass shown in (d) the full suite of targeted C_xH_y compound molecular masses (separate matrices exist for functionalized analytes, e.g. C_xH_yO, C_xH_yS) (Fig. 5). (e) Following calibration, replicate runs of the Macondo crude oil were characterized with the figure showing the mass distribution binned by carbon number and compound class. Note: The integration windows for each m/z are located based on n-alkanes in a DRO standard and known retention indices. Each individual ion in (d) is extracted with a mass accuracy error of 10 ppm which corresponds to extraction windows ranging from ± 0.0017 to ± 0.0045 m/z for C_{12} and C_{32} n-alkanes respectively.

ics (DBE $\geq$ 4) primarily ionize as $[M+H]^+$ via proton transfer and are quantified as such (Figure S3). We also observe differences in the propensity for fragmentation, which we minimized as much as possible by decreasing analyte temperature (via the transfer line temperature) coming into the ionization region [33].

Observed losses of the molecular ion due to fragmentation during ionization varied as a function of compound class and molecular size. Based on observations with simple standards and the relative response factors for each DBE in the NIST crude oil standard (Table S1 and S2), molecular ion fragmentation was greater for alkanes than for aromatic compounds. In addition, smaller alkanes (i.e. VOC range) were more likely to fragment than larger compounds (i.e. SVOC + range) due to having less orbital space to disperse the imposed charge. While there are considerable differences in both the fragmentation and ionization pathways between analytes, these differences are calibrated for using the NIST Macondo crude oil standard, which has known mass concentrations for each carbon number and DBE in Worton et al. (2015) that are confirmed against other external results [31]. We also observe some distribution in the product ions due to carbon isotopes (Figure S3), but this effect is automatically calibrated for if the standard(s) has a similar ^{12}C to ^{13}C distribution.

Using these calibrations, the total peak area for each target parent ion (i.e. molecular formula) can be summed, and their calculated mass abundances can determine the relative contribution of different carbon numbers and compound classes to the composition of

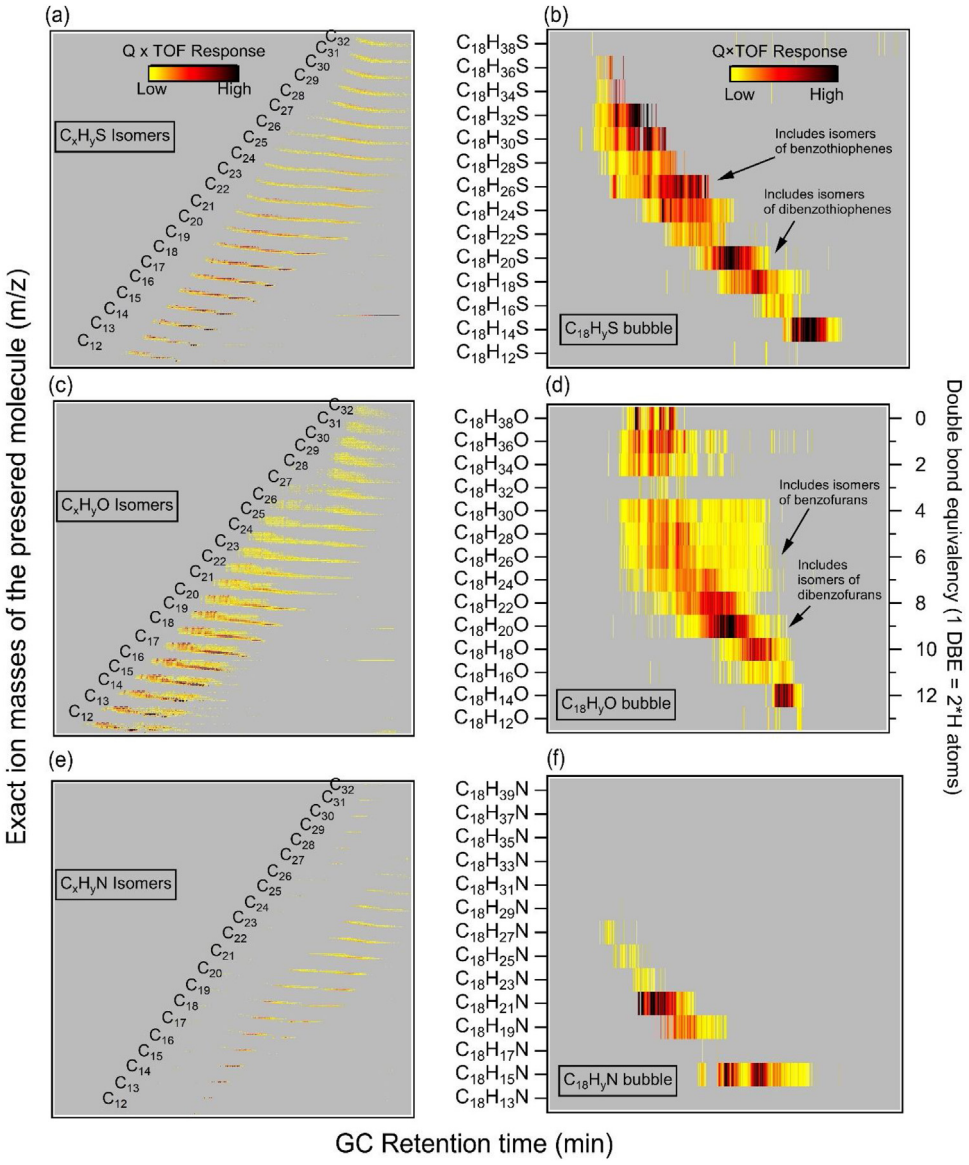

Fig. 5. Speciation of complex functionalized mixtures. (a) C_xH_yS, (c) C_xH_yO and (e) C_xH_yN functional group profiles from NIST crude oil standard in the C_{12}-C_{32} size range. Also shown are magnified C_{18} bubbles for each of the three functional groups in (b), (d) and (f) respectively. Note: The relative locations of compounds are tracked via retention indices determined from n-alkane standards.

the complex mixture. The sums of the peak areas for each $C_{\#}$ and DBE are shown in Fig. 4c for IVOCs and SVOCs (i.e. C_{12} to C_{28}) and are used for calibration to determine the response factors for each $C_{\#}$ and DBE. Fig. 4e shows the calibrated results of separate runs of the Macondo crude oil standard, with a distribution that is similar to previous analysis of Macondo crude oil [31]. Thus in future studies, these differences in response factors from fragmentation or ionization efficiency and product distributions are calibrated for using the extensive complex mixture calibration enabled by the NIST crude oil standard, supplemented by other simple mixture standards.

3.1.3. *Resolving functionalized compounds: oxygen-, sulfur-, and nitrogen-containing mixtures and other compound functionalities*

In addition to the C_xH_y hydrocarbons layer, we also observe a diversity of functionalized compounds containing oxygen, sulfur, and nitrogen atoms in crude oil and atmospheric samples (Figs. 5,6, S7 and S8 respectively). Each layer is further separated into their contributing molecular formulas in the same targeted way as the C_xH_y layer, across carbon numbers and series of molecular formulas (e.g. DBE for C_xH_yO) (Figs. 5). In the Macondo crude oil, we observed complex functionalized layers for C_xH_yS, C_xH_yO, and C_xH_yN for a long series of carbon numbers and spread across a range of molecular formulas as shown in Fig. 5. The authenticity and structure of compounds in these functionalized layers can be further validated or informed by their retention indices relative to n-alkanes in standards (i.e. diesel range organics (DRO)) or analyzed samples. In the crude oil, these include heteroatom-containing compounds with oxygen (e.g. furans), nitrogen, or reduced-sulfur (e.g. benzo- and dibenzo-thiophenes), most of which have been observed in previous studies of crude oil (Fig. 5) [48]. Future targeted data extraction on other samples is possible for any similar series of analytes (e.g. $C_xH_yNO_3$). These targeted approaches enable a data analysis/visualization and chemical speciation in a systematic, efficient, and comprehensive manner.

3.1.4. *Speciating environmental IVOCs, SVOCs, and LVOCs*

Complex airborne mixtures can be characterized using the framework that was discussed in Section 2.4 and validated with

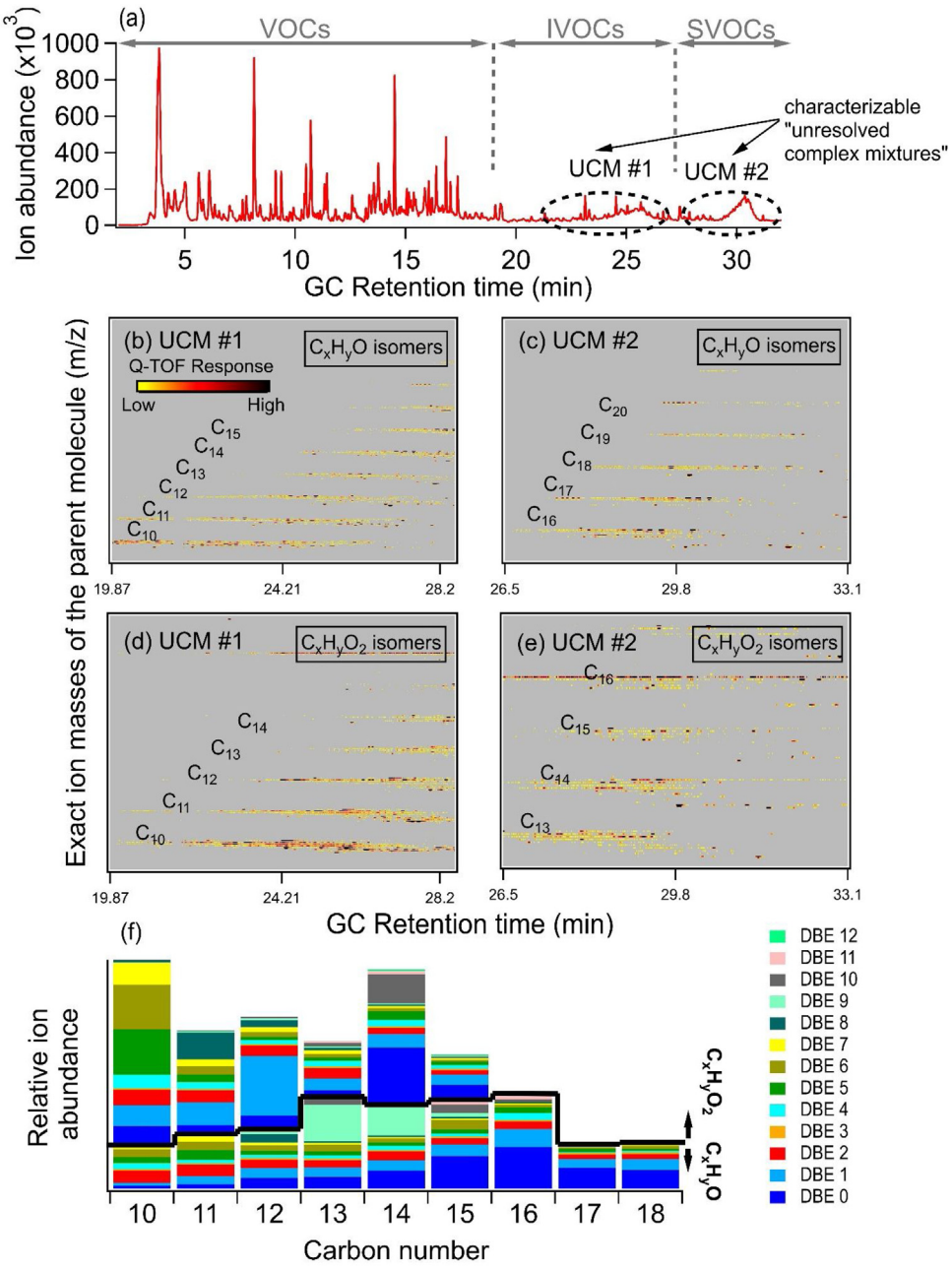

Fig. 6. A gas-phase offline sample collected from Manhattan in New York City in August 2018 analyzed using our integrated sampling-to-analysis system. (a) Total ion chromatogram (EI-MS). (b–e) Blank-subtracted C_xH_yO and $C_xH_yO_2$ layers show the composition of the two UCMs in the chromatogram. (f) Distribution of DBEs within the C_xH_yO and $C_xH_yO_2$ UCMs. Notes: The ion masses in the y-axes of (b–e) are not identical. The long band in (d–e) is a known contaminant, also present in the blank. Close-ups of the $C_{15}H_yO$ and $C_{15}H_yO_2$ bubbles are shown as examples in Figure S11.

the crude oil standard. This approach allows for efficient targeted characterization of environmental samples across a wide range of potential molecular structures including C_xH_y, C_xH_yO, $C_xH_yO_2$, C_xH_yS, C_xH_yN, C_xH_yON and $C_xH_yO_2N$, while chromatographic separation provides further constraints across GC retention time space, which enables the use of retention indices as a way to confirm compound identities.

We collected and analyzed a set of urban gas- and aerosol-phase ambient samples from Atlanta and New York City to test the system with our targeted approach (Figs. 6, 7, S7, S8 and S11). These samples show diverse analytes (C_xH_y and functionalized compounds) ranging from VOCs up to LVOCs. Examples of functionalized, gas-phase IVOCs measured in 6 L air samples via our integrated sampling-to-analysis system include aromatic ketones (e.g. $C_{13}H_{16}O$, $C_{14}H_{18}O$) and other cyclic and acyclic carbonyls (e.g. $C_9H_{14}O$) (Figures S7). Similarly, in one NYC sample, a series of oxygenated compounds are found in the $C_xH_yO_2$ layer, which include formulas for C_{14}-C_{21} cyclic esters and acids, and their isomers (Figure S8). To increase the sensitivity and comprehensive complex mixture speciation, subsequent ambient samples for APCI will be collected at higher flow rates and sample volumes (e.g. 25–50 L) as demonstrated in Sheu et al. [42].

A 22.5 L gas-phase sample from NYC shows a wide volatility range of analytes, including 2 UCMs comprised of oxygenated IVOCs-SVOCs containing 10–18 C atoms (Fig. 6). Both C_xH_yO and $C_xH_yO_2$ compounds are observed in the 2 UCMs, though C_xH_yO appears to be slightly more populated. A close-up evaluation of their carbon bubbles reveals a mix of compounds with 0–2 DBEs,

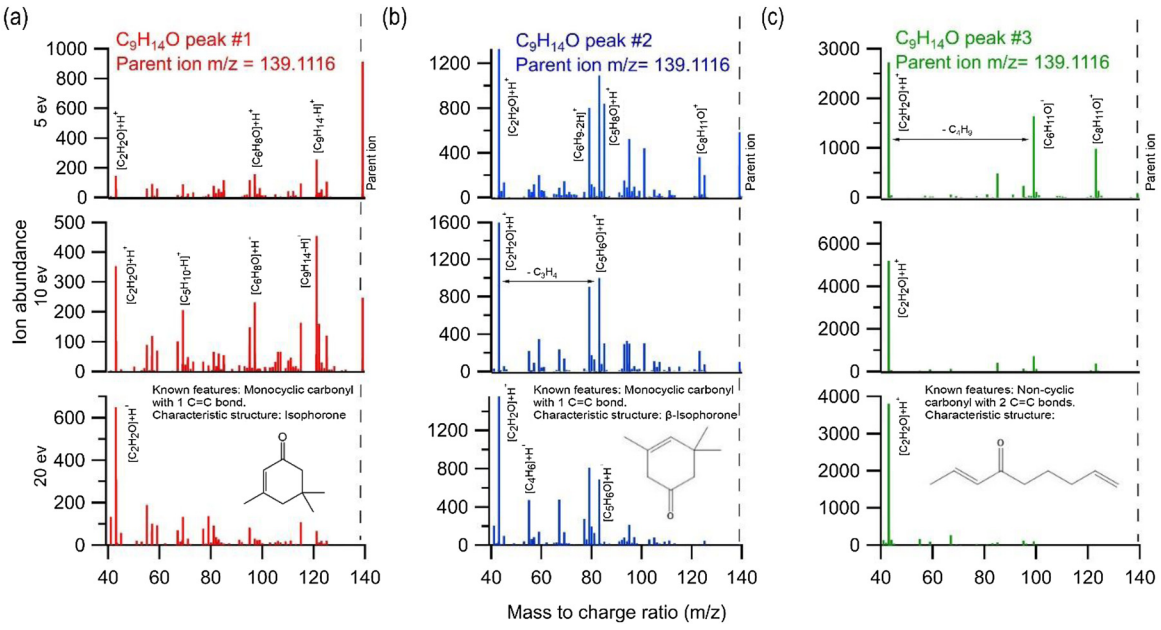

Fig. 7. Example of MS/MS analysis to differentiate isomers and characterize structural features using one adsorbent tube sample from near downtown Atlanta in Aug. 2017. Three unknown compounds were GC-separated and characterized by MS/MS at 3 different fragmentation energies (5, 10, 20 eV) and the MS/MS spectra are shown for each compound in (a)-(c) with the parent mass, notable fragments, and selected ion losses labeled. Each compound fragments differently at each energy in terms of degree and fragmentation patterns. The SIRIUS and CSI: Finger ID MS/MS structural identification tools are used to determine molecular features and characteristic structures shown in the bottom panels. Isophorone and β-isophorone (panels (a) and (b), respectively) are known species, while the structure in (c) is shown to illustrate the detected molecular features. For all 3, the structural features ID-ed are reported with high confidence based on the top, highest-scoring matches.

which represent linear and mono-/bi-cyclic oxygenates (Figs. 6f, S11). We also observe likely single-ring aromatic oxygenated compounds and their isomers on DBEs 4–6 and possible oxygenated PAHs on larger DBEs (Fig. 6f). This observation and characterization of oxygenated UCMs in the ambient atmosphere presents a valuable approach to evaluate transformations of gas- and particle-phase complex mixtures and SOA formation in future work. While the results in this paper are limited to the presentation of the application and its measurements in a limited number of samples, the observation of complex oxidized hydrocarbon mixtures is similar to a prior oxidation chamber study [29].

3.2. Routine tandem MS (MS/MS) for structural characterization of analytes

The use of GC–MS/MS for structural characterization can generate additional valuable information on the structural features present in a complex mixture or key analytes. We demonstrated the use of MS/MS with our integrated-sampling-to-analysis system to further characterize complex mixtures and differentiate between structural isomers. Future work using our integrated measurement system will apply this technique more widely across observed analytes, but here we show its capabilities with a subset of isomers.

In Fig. 7, we show a representative example with the targeted analysis of isophorone ($C_9H_{14}O$) found in gas-phase samples collected near downtown Atlanta GA, which the U.S. Environmental Protection Agency lists as a hazardous air pollutant. Isophorone is a widely-used solvent in printing, metal coating, synthesis, and some pesticides [49], and isomer-specific measurements of oxygenates like isophorone are growing in importance with the increased role of non-combustion emissions in air quality [39]. Here, 3 prominent isomers of $C_9H_{14}O$ were distinguished with a parent ion mass m/z of 139.1116 and 3 fully separate GC peaks. The MS/MS fragmentation at varying fragmentation energies (5, 10, 20 eV) reveals valuable information about the analytes' structures. The cyclic structure of the parent molecules in Fig. 7a-b require more energy to fragment in MS/MS, while the one in Fig. 7c breaks down completely into smaller fragments at even the lowest energy. Fig. 7 also shows examples of the elemental composition of the fragments as well as the ion losses between fragments. This information is used by automated MS/MS libraries and tools to suggest the structure and functionality of the analytes. For each individual GC peak, we applied the CSI: Finger ID algorithm on the average mass spectra of three collision energies to determine the molecular features present and the highest probability molecular structures [50].

This MS/MS approach is useful to determine prominent molecular features present in analytes, but there is uncertainty in the exact structural configuration due to similarities in MS/MS fragmentation between some regioisomers (i.e. positional isomers). The characteristic structures in Fig. 7a-b were predicted by the MS/MS analysis in SIRIUS/CSI: FingerID as isophorone and its very similar isomer β-isophorone. Their cyclic structures were consistent with the observed GC retention indices (NIST Chemistry WebBook). However, this MS/MS analysis alone is insufficient to definitively distinguish between the two. The potential molecular structure presented in Fig. 7c is less known and shown for the purposes of demonstrating the structural features that were identified in all the top MS/MS library results determined using CSI: FingerID, which has been shown to be the best for organic compound identification [45]. While the exact structure remains more uncertain, there is utility in knowing the key structural features. Differentiating between compounds like isophorone and the structure in Fig. 7c can have implications for dynamics and chemical reactivity in the atmosphere due to their significantly different chemical properties despite having the same molecular formula.

Future work with MS/MS in our integrated system will involve surveying and evaluating MS/MS libraries and tools as they evolve and applying multiple libraries to make conclusions more robust. Combining the top results to confirm key features and using other data like relative GC retention time will provide the strongest formula and structure identifications. Results will also be filtered based on exclusion criteria developed for this instrument in Ditto

et al. [20]. Depending on the specific samples and application, MS/MS will be applied in a hybrid targeted-untargeted approach, where both analytes of interest and the highest concentration untargeted analytes that surpass an abundance threshold (and are not on exclusion lists) will be characterized via MS/MS. However, when doing normal GC-TOF-focused characterization, the fraction of time spent on MS/MS must be managed to maintain a minimum scan rate for good GC peak shape and resolution. Therefore, focused MS/MS will be implemented on replicate samples (or injections) with more extensive targeted lists and lower untargeted abundance thresholds.

3.3. Routine direct-TOF analysis of gas-phase organic compound samples to directly measure analytes with low GC transmission efficiency

Many analytes (e.g. organic acids, organic nitrates) are difficult to analyze using gas chromatography due to being thermally labile or irreversibly adsorbing to the GC phase or other components in analytical systems. Yet, many of these compounds have been observed through careful design of GC systems [15,51]. Our supplemental direct-TOF technique provides the capability to detect and quantify such analytes with very high mass accuracy, while also analyzing samples through GC-TOF. This is particularly important for adsorbent tubes that cannot be easily analyzed by both GC-TOF and LC-TOF like filter extracts.

Here, we show the preliminary results from the direct-TOF addition to our TD-GC-Q-TOF system in a selected application, with further testing and adjustment to come in subsequent work. We tested our direct-TOF technique using the same crude oil standard for consistency, which is known to contain oxygen-, sulfur, and nitrogen-functionalized aliphatic and aromatic compounds [52,53]. Figure S6a shows the expectedly-unresolved total ion desorptogram of Macondo crude oil standard produced via direct-TOF. In Figure S6b, a selection of extracted ion desorptograms with a focus on functionalized compounds are shown from data analysis using the targeted analyte list developed for the GC-APCI-Q-TOF analysis. We observed a large number of low-abundance, chemically-identifiable species including parent ions of multi-oxygenated species and also fragments, which may be partially resolved through the addition of MS/MS in direct-TOF and a slower temperature ramp. Further, spiking with thermally-sensitive analytes (isotopically-labelled where possible) will be used to track losses to fragmentation during tube desorption in future work.

3.4. Conclusions and future work

We demonstrated our integrated sampling-to-analysis system designed for chemically-detailed offline sample analysis of atmospherically-relevant complex mixtures of gas- and particle-phase organic compounds, which included simultaneous hard and soft ionization MS, HR-TOF at 8 ± 2 ppm, and structural characterization via MS/MS. While the instrument is ready for application, key areas for further improvement include exploring alternative ion sources to minimize compound fragmentation during soft ionization; developing tools for faster, automated analysis of MS/MS data from complex organic mixtures; and further development of public MS/MS libraries and exclusion ion lists for quick identification of contaminants and artifacts. Elaboration of future work can be found in Section S3.

Acknowledgements

We would like to thank Nga (Sally) Ng and Taekyu Joo (Georgia Tech.) for collecting the sample used in Fig. 7. We thank National Science Foundation, grant number: AWD0001666 and the Humboldt foundation for support. We also thank Agilent Technologies for their assistance and collaboration with the APCI interface and the Q-TOF and AMCX for Inertium-coated parts. We also thank Juan de la Mora (Yale), Arthur Chan (U. Toronto) and Gabriel Isaacman-VanWertz (Virginia Tech.) for the helpful discussions and Igor code, and the New York State Department of Environmental Protection, Brian C. McDonald (NOAA) and Fred Moshary (CCNY) for their assistance during sample collection in NYC.

Appendix A. Supplementary data

Supplementary material related to this article can be found, in the online version, at doi:https://doi.org/10.1016/j.chroma.2019.03.037.

References

[1] Burden of Disease From Ambient and Household Air Pollution: Database Estimates, World Health Organization, 2015 (Accessed 2 July, 2015) http://www.who.int/phe/health_topics/outdoorair/databases/en/.
[2] C.A.I. Pope, D.W. Dockery, Health effects of fine particulate air pollution: lines that connect, J. Air Waste Manag. Assoc. 56 (2006) 709–742.
[3] D.S. Tkacik, A.A. Presto, N.M. Donahue, A.L. Robinson, Secondary organic aerosol formation from intermediate-volatility organic compounds: cyclic, linear, and branched alkanes, Environ. Sci. Technol. 46 (2012) 8773–8781, http://dx.doi.org/10.1021/es301112c.
[4] M. Hallquist, J.C. Wenger, U. Baltensperger, Y. Rudich, D. Simpson, M. Claeys, J. Dommen, N.M. Donahue, C. George, A.H. Goldstein, J.F. Hamilton, H. Herrmann, T. Hoffmann, Y. Iinuma, M. Jang, M.E. Jenkin, J.L. Jimenez, A. Kiendler-Scharr, W. Maenhaut, G. McFiggans, T.F. Mentel, A. Monod, A.S.H. Prevot, J.H. Seinfeld, J.D. Surratt, R. Szmigielski, J. Wildt, The formation, properties and impact of secondary organic aerosol: current and emerging issues, Atmos. Chem. Phys. 9 (2009) 5155–5236.
[5] J.J. Schauer, M.J. Kleeman, G.R. Cass, B.R.T. Simoneit, Measurement of emissions from air pollution sources. 1. C 1 through C 29 organic compounds from meat charbroiling, Environ. Sci. Technol. 33 (1999) 1566–1577, http://dx.doi.org/10.1021/es980076j.
[6] D. Craig Sykes, I. Ephraim Woods, Geoffrey D. Smith*, Tomas Baer, R.E. Miller, Thermal Vaporization-Vacuum Ultraviolet Laser Ionization Time-of-Flight Mass Spectrometry of Single Aerosol Particles, 2002, http://dx.doi.org/10.1021/AC011225A.
[7] J. Warnke, R. Bandur, T. Hoffmann, Capillary-HPLC-ESI-MS/MS method for the determination of acidic products from the oxidation of monoterpenes in atmospheric aerosol samples, Anal. Bioanal. Chem. 385 (2006) 34–45, http://dx.doi.org/10.1007/s00216-006-0340-6.
[8] A. Reinhardt, C. Emmenegger, B. Gerrits, C. Panse, J. Dommen, U. Baltensperger, R. Zenobi, M. Kalberer, Ultrahigh mass resolution and accurate mass measurements as a tool to characterize oligomers in secondary organic aerosols, Anal. Chem. 79 (2007) 4074–4082, http://dx.doi.org/10.1021/ac062425v.
[9] I. Kourtchev, I.P.O. 'connor, C. Giorio, S.J. Fuller, K. Kristensen, W. Maenhaut, J.C. Wenger, J.R. Sodeau, M. Glasius, M. Kalberer, Effects of anthropogenic emissions on the molecular composition of urban organic aerosols: an ultrahigh resolution mass spectrometry study, Atmos. Environ. 89 (2014) 525–532, http://dx.doi.org/10.1016/j.atmosenv.2014.02.051.
[10] M.P. Tolocka, M. Jang, J.M. Ginter, F.J. Cox, R.M. Kamens, M.V. Johnston, Formation of oligomers in secondary organic aerosol, Environ. Sci. Technol. 38 (2004) 1428–1434, http://dx.doi.org/10.1021/es035030r.
[11] D.R. Gentner, G. Isaacman, D.R. Worton, A.W.H. Chan, T.R. Dallmann, L. Davis, S. Liu, D.A. Day, L.M. Russell, K.R. Wilson, R. Weber, A. Guha, R.A. Harley, A.H. Goldstein, Elucidating secondary organic aerosol from diesel and gasoline vehicles through detailed characterization of organic carbon emissions, Proc. Natl. Acad. Sci. U. S. A. 109 (2012) 18318–18323, http://dx.doi.org/10.1073/pnas.1212272109.
[12] R.J. Yokelson, J.D. Crounse, P.F. Decarlo, T. Karl, S. Urbanski, E. Atlas, T. Campos, Y. Shinozuka, V. Kapustin, A.D. Clarke, A. Weinheimer, D.J. Knapp, D.D. Montzka, J. Holloway, P. Weibring, F. Flocke, W. Zheng, D. Toohey, P.O. Wennberg, C. Wiedinmyer, L. Mauldin, A. Fried, D. Richter, J. Walega, J.L. Jimenez, K. Adachi, P.R. Buseck, S.R. Hall, R. Shetter, Emissions from biomass burning in the Yucatan, Atmos. Chem. Phys. Atmos. Chem. Phys. 9 (2009) 5785–5812 (Accessed 7 February, 2018) www.atmos-chem-phys.net/9/5785/2009/.
[13] N.A. Freshour, K.K. Carlson, Y.A. Melka, S. Hinz, B. Panta, D.R. Hanson, Amine permeation sources characterized with acid neutralization and sensitivities of an amine mass spectrometer, Atmos. Meas. Tech. 7 (2014) 3611–3621, http://dx.doi.org/10.5194/amt-7-3611-2014.
[14] T.B. Nguyen, K.H. Bates, J.D. Crounse, R.H. Schwantes, X. Zhang, H.G. Kjaergaard, J.D. Surratt, P. Lin, A. Laskin, J.H. Seinfeld, P.O. Wennberg, Mechanism of the hydroxyl radical oxidation of methacryloyl peroxynitrate

(MPAN) and its pathway toward secondary organic aerosol formation in the atmosphere, Phys. Chem. Chem. Phys. 17 (2015) 17914–17926, http://dx.doi.org/10.1039/c5cp02001h.
[15] M.R. Beaver, J.M. St Clair, F. Paulot, K.M. Spencer, J.D. Crounse, B.W. LaFranchi, K.E. Min, S.E. Pusede, P.J. Wooldridge, G.W. Schade, C. Park, R.C. Cohen, P.O. Wennberg, Importance of biogenic precursors to the budget of organic nitrates: observations of multifunctional organic nitrates by CIMS and TD-LIF during BEARPEX 2009, Atmos. Chem. Phys. Atmos. Chem. Phys. 12 (2012) 5773–5785, http://dx.doi.org/10.5194/acp-12-5773-2012.
[16] G. Wang, Y. Sha, Z. Xu, J. Pan, Acetone chemical ionization mass spectrometry of monosaccharides, Anal. Chem. 57 (1985) 2283–2286, http://dx.doi.org/10.1021/ac00289a025.
[17] M. Riva, S.H. Budisulistiorini, Z. Zhang, A. Gold, J.D. Surratt, Chemical characterization of secondary organic aerosol constituents from isoprene ozonolysis in the presence of acidic aerosol, Atmos. Environ. 130 (2016) 5–13, http://dx.doi.org/10.1016/j.atmosenv.2015.06.027.
[18] M. Riva, S.H. Budisulistiorini, Y. Chen, Z. Zhang, E.L. D'ambro, X. Zhang, A. Gold, B.J. Turpin, J.A. Thornton, M.R. Canagaratna, J.D. Surratt, Chemical characterization of secondary organic aerosol from oxidation of isoprene hydroxyhydroperoxides, Environ. Sci. Technol. 50 (2016) 9889–9899, http://dx.doi.org/10.1021/acs.est.6b02511.
[19] E. Naegele, Making Your LC Method Compatible With Mass Spectrometry Technical Overview, 2011 (Accessed 9 August, 2018) https://www.agilent.com/cs/library/technicaloverviews/public/5990–7413EN.pdf.
[20] J. Ditto, E. Barnes, P. Khare, M. Takeuchi, T. Joo, A.A.T. Bui, J. Lee-Taylor, G. Eris, Y. Chen, B. Aumont, J.L. Jimenez, N.L. Ng, R.J. Griffin, D.R. Gentner, An omnipresent diversity and variability in the chemical composition of atmospheric secondary organic aerosol, Nat. Commun. Chem. 1 (75) (2018).
[21] G.J. Getzinger, M.P. O'Connor, K. Hoelzer, B.D. Drollette, O. Karatum, M.A. Deshusses, P.L. Ferguson, M. Elsner, D.L. Plata, Natural gas residual fluids: sources, endpoints, and organic chemical composition after centralized waste treatment in Pennsylvania, Environ. Sci. Technol. 49 (2015) 8347–8355, http://dx.doi.org/10.1021/acs.est.5b00471.
[22] R. Bahreini, M.D. Keywood, N.L. Ng, V. Varutbangkul, S. Gao, R.C. Flagan, J.H. Seinfeld, A.D.R. Worsnop, J.L. Jimenez, Measurements of secondary organic aerosol from oxidation of cycloalkenes, terpenes, and m-xylene using an aerodyne aerosol mass spectrometer, Environ. Sci. Technol. 39 (2005) 5674–5688, http://dx.doi.org/10.1021/ES048061A.
[23] T. Portolés, J.V. Sancho, F. Hernández, A. Newton, P. Hancock, Potential of atmospheric pressure chemical ionization source in GC-QTOF MS for pesticide residue analysis, J. Mass Spectrom. 45 (2010) 926–936, http://dx.doi.org/10.1002/jms.1784.
[24] T. Portolés, J.G.J. Mol, J.V. Sancho, F. Hernández, Use of electron ionization and atmospheric pressure chemical ionization in gas chromatography coupled to time-of-flight mass spectrometry for screening and identification of organic pollutants in waters, J. Chromatogr. A 1339 (2014) 145–153, http://dx.doi.org/10.1016/j.chroma.2014.03.001.
[25] A.W.H. Chan, G. Isaacman, K.R. Wilson, D.R. Worton, C.R. Ruehl, T. Nah, D.R. Gentner, T.R. Dallmann, T.W. Kirchstetter, R.A. Harley, J.B. Gilman, W.C. Kuster, J.A. De Gouw, J.H. Offenberg, T.E. Kleindienst, Y.H. Lin, C.L. Rubitschun, J.D. Surratt, P.L. Hayes, J.L. Jimenez, A.H. Goldstein, A.W.H. Chan, Detailed chemical characterization of unresolved complex mixtures in atmospheric organics: insights into emission sources, atmospheric processing, and secondary organic aerosol formation, J. Geophys. Res. Atmos. 118 (2013) 6783–6796, http://dx.doi.org/10.1002/jgrd.50533.
[26] D.R. Gentner, G. Isaacman, D.R. Worton, A.W.H. Chan, T.R. Dallmann, L. Davis, S. Liu, D.A. Day, L.M. Russell, K.R. Wilson, R. Weber, A. Guha, R.A. Harley, A.H. Goldstein, Elucidating secondary organic aerosol from diesel and gasoline vehicles through detailed characterization of organic carbon emissions, Proc. Natl. Acad. Sci. U. S. A. 109 (2012) 18318–18323, http://dx.doi.org/10.1073/pnas.1212272109.
[27] S. Mitschke, A. Werner Welthagen, R. Zimmermann, Comprehensive gas chromatography–time-of-flight mass spectrometry using soft and selective photoionization techniques, Anal. Chem. 78 (2006) 6364–6375, http://dx.doi.org/10.1021/AC060531R.
[28] J. Schnelle-Kreis, W. Welthagen, M. Sklorz, R. Zimmermann, Application of direct thermal desorption gas chromatography and comprehensive two-dimensional gas chromatography coupled to time of flight mass spectrometry for analysis of organic compounds in ambient aerosol particles, J. Sep. Sci. 28 (2005) 1648–1657, http://dx.doi.org/10.1002/jssc.200500120.
[29] G. Isaacman, A.W.H. Chan, T. Nah, D.R. Worton, C.R. Ruehl, K.R. Wilson, A.H. Goldstein, Heterogeneous OH oxidation of motor oil particles causes selective depletion of branched and less cyclic hydrocarbons, Environ. Sci. Technol. 46 (2012) 10632–10640.
[30] K.A.S. Goodman-Rendall, Y.R. Zhuang, A. Amirav, A.W.H. Chan, Resolving detailed molecular structures in complex organic mixtures and modeling their secondary organic aerosol formation, Atmos. Environ. 128 (2016) 276–285, http://dx.doi.org/10.1016/j.atmosenv.2016.01.006.
[31] D.R. Worton, H. Zhang, G. Isaacman-VanWertz, A.W.H. Chan, K.R. Wilson, A.H. Goldstein, Comprehensive chemical characterization of hydrocarbons in NIST standard reference material 2779 gulf of Mexico crude oil, Environ. Sci. Technol. 49 (2015) 13130–13138, http://dx.doi.org/10.1021/acs.est.5b03472.
[32] D.R. Worton, G. Isaacman, D.R. Gentner, T.R. Dallmann, A.W.H. Chan, C. Ruehl, T.W. Kirchstetter, K.R. Wilson, R.A. Harley, A.H. Goldstein, Lubricating oil dominates primary organic aerosol emissions from motor vehicles, Environ. Sci. Technol. 48 (2014) 3698–3706, http://dx.doi.org/10.1021/es405375j.
[33] G. Isaacman, K.R. Wilson, A.W.H. Chan, D.R. Worton, J.R. Kimmel, T. Nah, T. Hohaus, M. Gonin, J.H. Kroll, D.R. Worsnop, A.H. Goldstein, Improved resolution of hydrocarbon structures and constitutional isomers in complex mixtures using gas chromatography-vacuum ultraviolet-mass spectrometry, Anal. Chem. 84 (2012) 2335–2342, http://dx.doi.org/10.1021/ac2030464.
[34] R. Zimmermann, W. Welthagen, T. Gröger, Photo-ionisation mass spectrometry as detection method for gas chromatography optical selectivity and multidimensional comprehensive separations, J. Chromatogr. A 1184 (2008) 296–308, http://dx.doi.org/10.1016/j.chroma.2007.08.081.
[35] R. Zimmermann, F. Mühlberger, K. Fuhrer, M. Gonin, W. Welthagen, An ultracompact photo-ionization time-of-flight mass spectrometer with a novel vacuum ultraviolet light source for on-line detection of organic trace compounds and as a detector for gas chromatography, J. Mater. Cycles Waste Manag. 10 (2008) 24–31, http://dx.doi.org/10.1007/s10163-007-0194-9.
[36] L. Vogt, T. Gröger, R. Zimmermann, Automated compound classification for ambient aerosol sample separations using comprehensive two-dimensional gas chromatography-time-of-flight mass spectrometry, J. Chromatogr. A 1150 (2007) 2–12, http://dx.doi.org/10.1016/j.chroma.2007.03.006.
[37] J. Laskin, A. Laskin, P.J. Roach, G.W. Slysz, G.A. Anderson, S.A. Nizkorodov, D.L. Bones, L.Q. Nguyen, High-resolution desorption electrospray ionization mass spectrometry for chemical characterization of organic aerosols, Anal. Chem. 82 (2010) 2048–2058, http://dx.doi.org/10.1021/ac902801f.
[38] J.F. Hunter, D.A. Day, B.B. Palm, R.L.N. Yatavelli, A.W.H. Chan, L. Kaser, L. Cappellin, P.L. Hayes, E.S. Cross, A.J. Carrasquillo, P. Campuzano-Jost, H. Stark, Y. Zhao, T. Hohaus, J.N. Smith, A. Hansel, T. Karl, A.H. Goldstein, A. Guenther, D.R. Worsnop, J.A. Thornton, C.L. Heald, J.L. Jimenez, J.H. Kroll, Comprehensive characterization of atmospheric organic carbon at a forested site, Nat. Geosci. (2017), http://dx.doi.org/10.1038/ngeo3018.
[39] P. Khare, D.R. Gentner, Considering the future of anthropogenic gas-phase organic compound emissions and the increasing influence of non-combustion sources on urban air quality, Atmos. Chem. Phys. 18 (2018) 5391–5413, http://dx.doi.org/10.5194/acp-18-5391-2018.
[40] D.R. Gentner, S.H. Jathar, T.D. Gordon, R. Bahreini, D.A. Day, I. El Haddad, P.L. Hayes, S.M. Pieber, S.M. Platt, J. de Gouw, A.H. Goldstein, R.A. Harley, J.L. Jimenez, A.S.H. Prévôt, A.L. Robinson, Review of urban secondary organic aerosol formation from gasoline and diesel motor vehicle emissions, Environ. Sci. Technol. 51 (2017) 1074–1093, http://dx.doi.org/10.1021/acs.est.6b04509.
[41] C. Zuth, A.L. Vogel, S. Ockenfeld, R. Huesmann, T. Hoffmann, Ultrahigh-Resolution Mass Spectrometry in Real Time: Atmospheric Pressure Chemical Ionization Orbitrap Mass Spectrometry of Atmospheric Organic Aerosol, 2018, http://dx.doi.org/10.1021/acs.analchem.8b00671.
[42] R. Sheu, A. Marcotte, P. Khare, S. Charan, J. Ditto, D.R. Gentner, Advances in offline approaches for speciated measurements of trace gas-phase organic compounds via an integrated sampling-to-analysis system, J. Chromatogr. A (2018), submitted.
[43] R.E. Martinez, B.J. Williams, Y. Zhang, D. Hagan, M. Walker, N.M. Kreisberg, S.V. Hering, T. Hohaus, J.T. Jayne, D.R. Worsnop, Development of a volatility and polarity separator (VAPS) for volatility- and polarity-resolved organic aerosol measurement, Aerosol Sci. Technol. 50 (2016) 255–271, http://dx.doi.org/10.1080/02786826.2016.1147645.
[44] E.M. Thurman, I. Ferrer, The isotopic mass defect: a tool for limiting molecular formulas by accurate mass, Anal. Bioanal. Chem. 397 (2010) 2807–2816, http://dx.doi.org/10.1007/s00216-010-3562-6.
[45] K. Dührkop, H. Shen, M. Meusel, J. Rousu, S. Böcker, Searching molecular structure databases with tandem mass spectra using CSI: FingerID, Proc. Natl. Acad. Sci. U. S. A. 112 (2015) 12580–12585, http://dx.doi.org/10.1073/pnas.1509788112.
[46] E.L. Schymanski, C. Ruttkies, M. Krauss, C. Brouard, T. Kind, K. Dührkop, F. Allen, A. Vaniya, D. Verdegem, S. Böcker, J. Rousu, H. Shen, H. Tsugawa, T. Sajed, O. Fiehn, B. Ghesquière, S. Neumann, Critical assessment of small molecule identification 2016: automated methods, J. Cheminform. 9 (2017), http://dx.doi.org/10.1186/s13321-017-0207-1.
[47] S. Böcker, M.C. Letzel, Z. Lipták, A. Pervukhin, SIRIUS: decomposing isotope patterns for metabolite identification, Bioinforma. Orig. Pap. 25 (2009) 218–224, http://dx.doi.org/10.1093/bioinformatics/btn603.
[48] P.W. Sammarco, S.R. Kolian, R.A.F. Warby, J.L. Bouldin, W.A. Subra, S.A. Porter, Distribution and concentrations of petroleum hydrocarbons associated with the BP/Deepwater Horizon Oil Spill, Gulf of Mexico, Mar. Pollut. Bull. 73 (2013) 129–143, http://dx.doi.org/10.1016/j.marpolbul.2013.05.029.
[49] Hazard Summary, 2000 (Accessed 4 July, 2018) https://www.epa.gov/sites/production/files/2016-09/documents/isophorone.pdf.
[50] S. Wolf, S. Schmidt, M. Müller-Hannemann, S. Neumann, In silico fragmentation for computer assisted identification of metabolite mass spectra, BMC Bioinformatics 11 (2010), http://dx.doi.org/10.1186/1471-2105-11-148.
[51] B.J. Williams, J.T. Jayne, A.T. Lambe, T. Hohaus, J.R. Kimmel, D. Sueper, W. Brooks, L.R. Williams, A.M. Trimborn, R.E. Martinez, P.L. Hayes, J.L. Jimenez, N.M. Kreisberg, S.V. Hering, D.R. Worton, A.H. Goldstein, D.R. Worsnop, The first combined thermal desorption aerosol gas chromatograph - Aerosol mass spectrometer (TAG-AMS), Aerosol Sci. Technol. 48 (2014) 358–370, http://dx.doi.org/10.1080/02786826.2013.875114.

[52] D.L. Valentine, E.B. Overton, T.L. Wade, J.R. Radović, B.M. Meyer, M.S. Miles, S.R. Larter, Chemical composition of Macondo and other crude oils and compositional alterations during oil spills introduction: what are crude oils? Oceanography 29 (2016) 50–63 (accessed June 22, 2018) https://tos.org/oceanography/assets/docs/29-3_overton.pdf.

[53] L.A. Stanford, S. Kim, G.C. Klein, D.F. Smith, A. Ryan, P. Rodgers, Alan G. Marshall, Identification of water-soluble heavy crude oil organic-acids, bases, and neutrals by electrospray ionization and field desorption ionization fourier transform ion cyclotron resonance mass spectrometry, Environ. Sci. Technol. 41 (2007) 2696–2702, http://dx.doi.org/10.1021/ES0624063.